



저작자표시-비영리-변경금지 2.0 대한민국

이용자는 아래의 조건을 따르는 경우에 한하여 자유롭게

- 이 저작물을 복제, 배포, 전송, 전시, 공연 및 방송할 수 있습니다.

다음과 같은 조건을 따라야 합니다:



저작자표시. 귀하는 원저작자를 표시하여야 합니다.



비영리. 귀하는 이 저작물을 영리 목적으로 이용할 수 없습니다.



변경금지. 귀하는 이 저작물을 개작, 변형 또는 가공할 수 없습니다.

- 귀하는, 이 저작물의 재이용이나 배포의 경우, 이 저작물에 적용된 이용허락조건을 명확하게 나타내어야 합니다.
- 저작권자로부터 별도의 허가를 받으면 이러한 조건들은 적용되지 않습니다.

저작권법에 따른 이용자의 권리는 위의 내용에 의하여 영향을 받지 않습니다.

이것은 [이용허락규약\(Legal Code\)](#)을 이해하기 쉽게 요약한 것입니다.

[Disclaimer](#)

공학석사 학위논문

**Effect of diffusion of disperse dyes
inside the polymer matrix on the
kinetics of dyeing of PET using
supercritical CO₂**

고분자 매트릭스 내 분산염료의 확산이
초임계이산화탄소를 이용한 PET의
염색속도론에 미치는 영향

2021년 2월

서울대학교 대학원

화학생물공학부

김 동 준

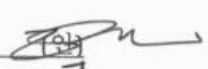


**Effect of diffusion of disperse dyes inside the
polymer matrix on the kinetics of dyeing of PET
using supercritical CO₂**

지도교수 이 윤 우

이 논문을 공학석사 학위논문으로 제출함
2021 년 2 월

서울대학교 대학원
화학생명공학부
김 동 준

김동준의 공학석사 학위논문을 인준함
2021 년 2 월

위원장	이 종 민	
부위원장	이 윤 우	
위 원	이 원 보	

Abstract

Effect of diffusion of disperse dyes inside the polymer matrix on the kinetics of dyeing of PET using supercritical CO₂

Dongjoon Kim

School of Chemical and Biological Engineering

Seoul National University

Supercritical dyeing (SCD) of PET using carbon dioxide with three disperse dyes (Disperse Yellow 54, Disperse Yellow 211, and Disperse Blue 359) was studied under 393 K, 250 bar. To find the governing factor that is consistent with the dyeing kinetics, dissolution rate, solubility of dyes, solubility parameter, and dye uptake were measured and compared. Dye uptake showed proportionality to $\sqrt{D_{AB}t}$ which implied SCD process not only occurred in a similar manner as the unsteady-state diffusion in semi-infinite medium but was also limited by the diffusion step. From the hypothesis that diffusion was the rate determining step for the SCD process, governing equation for the dye uptake was achieved and the expected outcomes from the equation were compared with the experimental results. It was observed from the comparison that the governing equation overestimated the dye uptake and thus, the dyeing rate for all three dyes of use. Deviation of the experimental values from the theoretical ones could have been the result of low concentration of the dyes in the scCO₂ when the SCD process begun. The governing equation was obtained using the assumption that the scCO₂ is saturated with dyes at $t = 0$ or to have dye concentration of C_0 . From the dissolution rate measurement, however, the concentration of the dyes in the scCO₂ did not reach the maximum value until around 20 minutes into dissolution which suggested that for all of the SCD processes, dye concentration was not at the maximum in the beginning but rather increased to the value after some time span. Lower concentration of the dyes at the fabric surface at $t = 0$, which was caused by slow dissolution rate, may have caused

the deviations of the data. To test the hypothesis, the governing equation was plotted with the initial values C_0 or the saturation concentration, $0.75C_0$, and $0.50C_0$ and the resulting curves were compared with the experimental results. It was shown that for short dyeing time, the experimental results match well with the curves obtained from either $0.75C_0$ or $0.50C_0$ whereas the experimental results for long dyeing time fitted better with the curve from C_0 . The observation, therefore, matched the assumption that the deviation was caused by the lower C_0 which resulted from slow dissolution rate of dyes into scCO_2 . Apart from the deviation, the governing equation seemed to predict the dye uptake or the dyeing rate for the overall SCD process well and the equation can be used to predict the dyeing kinetics of the untested dyes.

Keywords: Supercritical dyeing, disperse dye, PET, dyeing kinetics

Student Number: 2017-25711

Contents

Contents.....	iv
Chapter 1. Introduction.....	8
1.1 Research background	8
1.1.1 Supercritical fluid	10
1.1.2 Supercritical dyeing process	14
1.2 Selection of fabric.....	16
1.3 Disperse dyes	18
1.4 Aim of the study	20
Chapter 2. Experimental	21
2.1 Materials	21
2.2 Apparatus for dissolution of dyes into scCO ₂	22
2.3 Apparatus for supercritical dyeing.....	25
2.4 Apparatus for extraction of impregnated dye	26
2.5 Analytical methods.....	28
2.5.1 Measurement of the dissolution rate and solubility	28
2.5.2 Measurement of the dye uptake	29
Chapter 3. Results and discussion	30
3.1 Dye uptake	30
3.1.1 Solvent selection for soxhlet extraction	32
3.2 Calculation of the solubility parameter, δ	33
3.2.1 Dissolution of dyes into CO ₂	35
3.2.2 Mass transfer to polymer surface	38
3.3 Diffusion of dyes inside the polymer matrix	40
Chapter 4. Conclusion.....	49
Bibliography	52
국 문 초 록	55

List of Tables

Table 1.	Physical properties of liquid, gas, and supercritical fluid.....	12
Table 2.	Solubility of parameter, δ , of scCO ₂ , PET, DY54, DY211, and DB359.....	33
Table 3.	Solubility of disperse dyes in scCO ₂ at 393 K, 250 bar.....	38

List of Figures

Figure 1.	Phase diagram of CO ₂ . Above the critical point (●), fluid exists in the supercritical phase which is in the shaded area of the supercritical region.....	11
Figure 2.	Schematic diagram of the overall supercritical dyeing process.....	14
Figure 3.	Molecular structures of PET.....	16
Figure 4.	Molecular structures of (a) DY54, (b) DY211, and (c) DB359.....	18
Figure 5.	In-situ UV-Vis apparatus for measurement of dissolution rate and solubility of dyes into scCO ₂	23
Figure 6.	Soxhlet extractor used to extract the impregnated dye inside the PET at various time..	26
Figure 7.	Dyeing rate for various dyes at 393 K & 250 bar from 0 to 180 min. DY54 (◆), DY211 (●), and DB359 (■) were assumed to be fully saturate the fabric at 180 min and the concentration at this time was defined as equilibrium dye uptake.....	30
Figure 8.	In-situ UV-Vis Spectrophotometer for the measurement of solubility and dissolution rate at 393 K, 250 bar.....	35
Figure 9.	Dissolution rate of disperse dyes in scCO ₂ measured from in-situ UV-Vis Spectrophotometer at 393 K, 250 bar. scCO ₂ was assumed to be fully saturated with DY54 (—), DY211 (—), and DB359 (—) prior to 25 min.....	36
Figure 10.	Correlation between the dye uptake and $(D_{AB}t)^{1/2}$ for DY54 (◆), DY211 (●), and DB359 (■) at 393 K, 250 bar from 0 to 180 min.....	41
Figure 11.	SEM image of the PET used throughout the experiments.....	44
Figure 12.	Rate of dyeing for DY54. Expected values from the governing equation and experimental values of DY54 (◆) are plotted. The solid line represents the expected results for C_0 and the other two dashed lines for $0.75C_0$ and $0.5C_0$ respectively.....	45
Figure 13.	Rate of dyeing for DY211. Expected values from the governing equation and experimental values of DY211 (●) are plotted. The solid line represents the expected results for C_0 and the other two dashed lines for $0.75C_0$ and $0.5C_0$ respectively.....	46

Figure 14. Rate of dyeing for DB359. Expected values from the governing equation and experimental values of DB359 (■) are plotted. The solid line represents the expected results for C_0 and the other two dashed lines for $0.75C_0$ and $0.5C_0$ respectively.....47

Chapter 1. Introduction

1.1 Research background

For a very long time, dyeing process has been the essential part of the textile industry. Majority of the cases, conventional aqueous dyeing which uses water as the medium was adopted as the go-to technology. Conventional aqueous dyeing, however, comes with massive production of waste water from processes such as dyeing and printing. According to The World Bank, the waste water that comes from dyeing and printing industries account for 17~20% of the total industrial water pollution. [1] For a textile mill that produces 8000 kg of fabric per day, around 1.6 million liters of water is consumed daily. [1] Waste water from the dyeing process not only contains various toxic chemicals that were used as additives or surfactants but also lower the photosynthetic ability of plants and lower the oxygen concentration in the water which ultimately have negative influence on the microorganisms.

In order to account for the negative aspect of the conventional aqueous dyeing, supercritical dyeing which uses carbon dioxide instead of water has

been proposed as an alternative dyeing technology. In the late 1980s, supercritical dyeing was first proposed by Professor Schollmeyer and his team and been studied by many other groups ever since. [2] Previous studies include supercritical dyeing processes for both synthetic and natural fiber where dissolution of dyes into scCO_2 , interaction between scCO_2 and polymer, and equilibrium dye partitioning between scCO_2 and fiber were examined separately. Despite extensively studied, not many researches had been done on the supercritical dyeing process where the dyeing kinetics was studied for the whole dyeing process rather than a specific step such as dissolution or the diffusion. The goal of this study was to find a way to predict the dyeing kinetics with a simple one or two experimentations without having to examine each step of the dyeing process separately.

1.1.1 Supercritical fluid

A form of phase where a substance exists which usually is one of solid, gas, or vapor, depends on the temperature and pressure as shown in Figure 1. It is considered that a substance is in the supercritical phase when the temperature and pressure exceeds the critical values, known as the critical point. Fluid where the reaction conditions are over the critical point is called supercritical fluid (SCF) and SCF shows deviations in the physical properties from liquid and gases. [3] As shown in Table 1, SCF has density similar to liquid while having a wider range compared to either liquid or gas which is a representation of the special thermos-physical properties of SCF. In contrast to gas where increase in pressure leads to negligible change in density, pressure increase for SCF can not only change the density easily but also increase the dissolution power of the fluid. In other words, in the supercritical region, fluid has both the mobility of a gas and the solvation power of a liquid. Due to the solvation power of the SCF and the fact that the physical properties can be delicately controlled by varying temperature and pressure, SCF has been adopted in many areas such as pharmaceutical, food processing, textile processing, and more.[2,4,5] Among

all others, carbon dioxide is one of the most widely used SCFs for various applications such as supercritical fluid extraction, supercritical dyeing, and even energy generation through nuclear reactors where scCO_2 Brayton cycle is used.[6,7] Supercritical carbon dioxide (scCO_2) has few advantages over others such as non-flammability, cheap price, mild critical conditions (304 K, 7.38 MPa), and environmentally benign features.

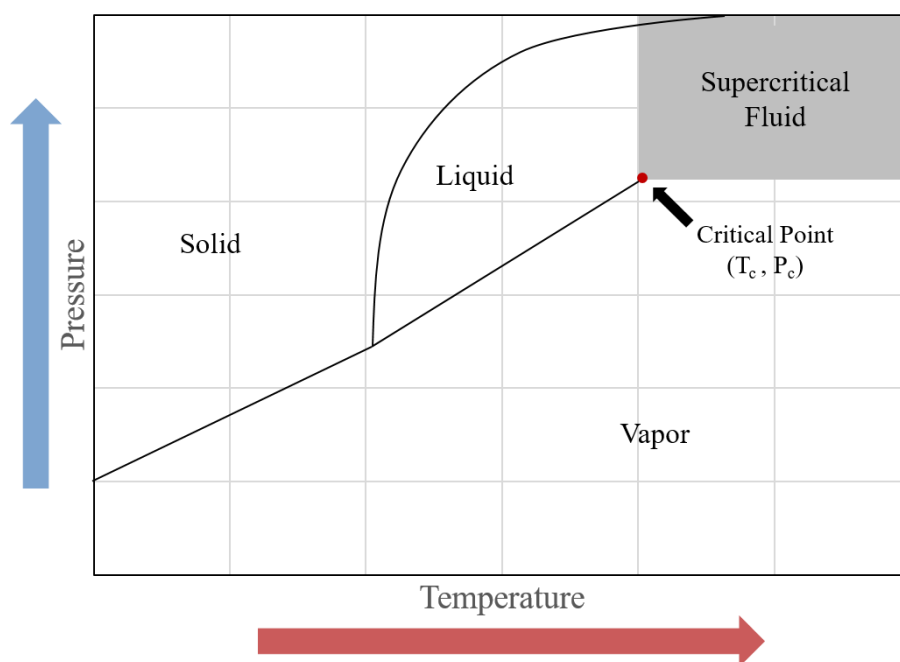


Figure 1. Phase diagram of CO₂. Above the critical point (●), fluid exists in the supercritical phase which is in the shaded area of the supercritical region.

Table 1.

Physical properties of liquid, gas, and supercritical fluid. [3]

	Liquid	Gas	SCF
Density [kg/m^3]	1000	$0.6 \sim 1$	$200 \sim 900$
Viscosity [$\mu\text{Pa}\cdot\text{s}$]	10^{-3}	10^{-5}	$10^{-5} \sim 10^{-4}$
Diffusion coefficient [m^2/s]	$<10^{-9}$	10^{-5}	$10^{-8} \sim 10^{-7}$
Heat conductivity [W/mK]	$<10^{-1}$	10^{-3}	$10^{-3} \sim 10^{-1}$

1.1.2 Supercritical dyeing process

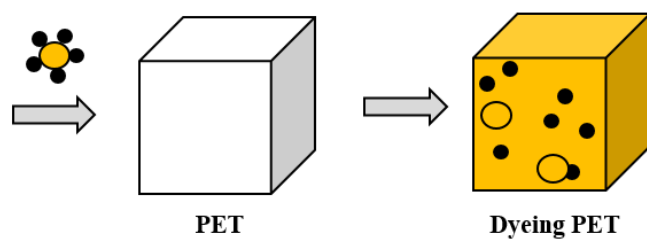
Supercritical dyeing (SCD) processes can be classified into three major steps as shown graphically in Figure 2: dissolution of the dye stuff into the scCO_2 , mass transfer of the dye- CO_2 mixture to the surface of the textile, and last but not least, diffusion of the dye inside the polymer matrix. Studies on SCD technology have been done by many researchers using not only natural fabrics such as cotton and wool but also synthetic fabrics including polyethylene terephthalate (PET), polyamide, and polypropylene [8-12]

SCD processes holds numerous advantages compared to the conventional aqueous dyeing. The most significant one is the absence of the wastewater after the process is finished. The absence of wastewater implies that the SCD process is not only environmentally friendly but also drying stage after the process is unnecessary which in turn will save the heat energy and the expenses that would have been invested into designing the drying apparatus. Also, majority of the dyes will be prepared to react with the fabric because the dyes will not be hydrolyzed during the process. [13]

Dissolution of dyes into scCO₂



Impregnation of dyes into PET



Recovery of excess dyes by depressurization

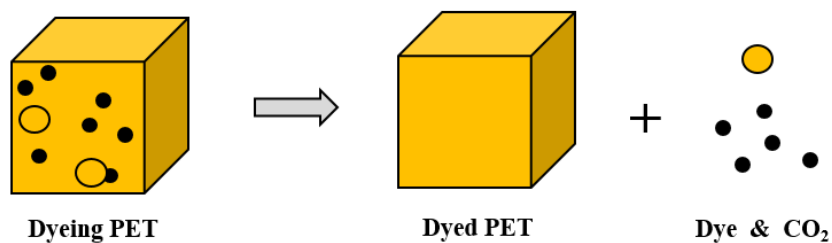


Figure 2. Schematic diagram of the overall supercritical dyeing process.

1.2 Selection of fabric

Among many fabrics, PET was most extensively studied in the SCD field for few reasons such as excellent physical properties and massive usage of PET worldwide. Residential and industrial areas have high usage of PET due to its good tensile, impact strength, low cost, and high thermal stability. [13-15] In 2015, more than 18 million tons of PET were manufactured worldwide which was around 7% of the total plastic production of 269 million tons. [16]

Carbon dioxide, having numerous benefits including non-flammability, environmentally green, cheap, and non-polar properties, is adopted in SCD processes. Apart from the previously mentioned merits, CO₂ offers an additional feature that is essential to SCD processes: swelling. Swelling of the PET results from the plasticization effect caused by the movement of CO₂ molecules into the amorphous portion of the polymer matrix. As CO₂ molecules enter the system, segmental chain mobility and free volume inside the matrix are increased. Swelling caused by CO₂ sorption not only reduces the glass transition temperature of the polymer but also known to enhance the dyeing. [8,17]

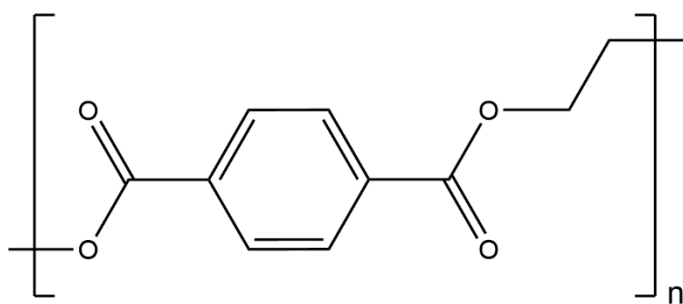
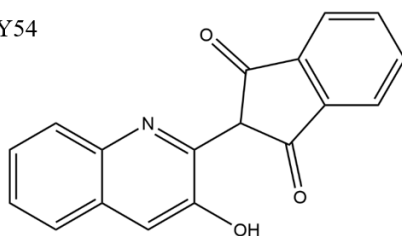


Figure 3. Molecular structures of PET

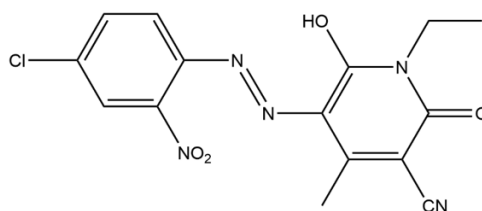
1.3 Disperse dyes

To understand the SCD processes in a deeper way, studies on disperse dyes were carried by many research groups where dyes were classified into polarity, molecular structure, or others. Molecular structure and functional groups of disperse dyes is known to affect not only the diffusion inside the polymer but also the dissolution into scCO₂. [9,18] In order to observe any possible influence of the molecular structure on the overall dyeing process, disperse dyes with three different molecular structure, Disperse Yellow 54 (DY54), Disperse Yellow 211 (DY211), and Disperse Blue 359 (DB359) were chosen. The molecular structure and other properties of the dyes of interest are shown in Figure 4.

(a) DY54



(b) DY211



(c) DB359

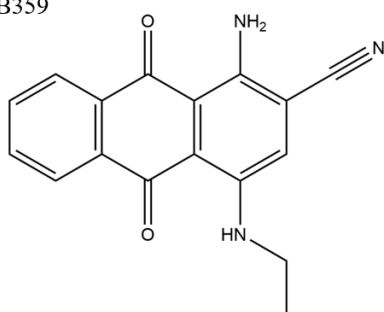


Figure 4. Molecular structures of (a) DY54, (b) DY211, and (c) DB359.

1.4 Aim of the study

The aim of this study is to find the factor that affects the overall SCD process in the same way no matter the identity of the disperse dye. There exist numerous studies on the dissolution of dyes into scCO₂ or the diffusion of the dyes inside the polymer matrix alone. Not many, however, have attempted to find a factor that can be used for the overall SCD process rather than only dissolution or diffusion step. To achieve the goal, following objectives were proposed.

1. To observe the effect of dyes to the dissolution step, dissolution rate and solubility of each dyes into scCO₂ were measured.
2. The overall rate of dyeing was measured experimentally and the results were compared with factors that could affect the overall process such as diffusion coefficient of dye inside the PET, solubility parameter differences, and equilibrium dye uptake.
3. From the experimental data, governing equation for the overall SCD process can be obtained. Using this equation, dyeing kinetics of the untested dyes can be predicted given the reaction conditions are identical.

Chapter 2. Experimental

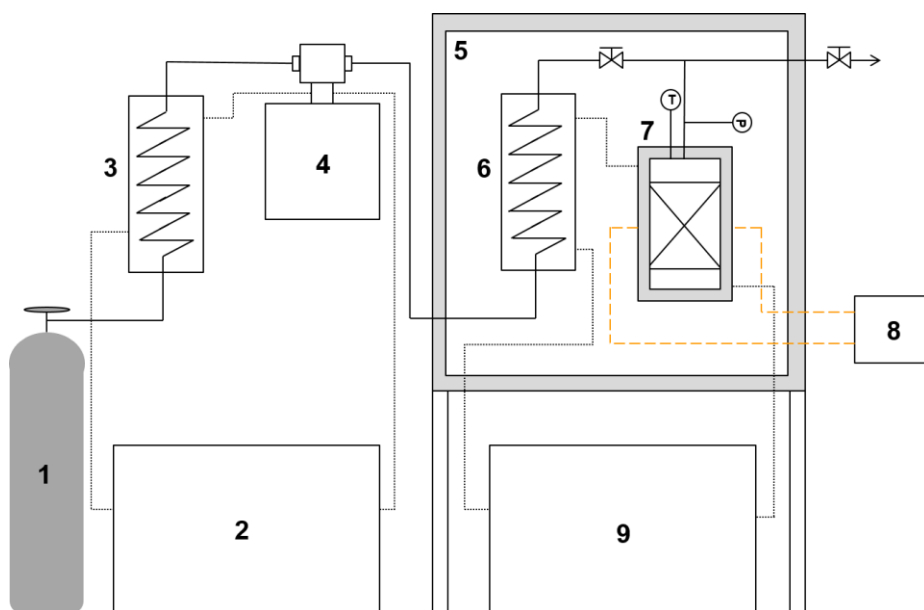
2.1 Materials

Carbon dioxide (99.9%) and nitrogen (99.999%, CAS No. 7727-37-9) were acquired from Hyupshin Gas Industry. Acetone (99.5% & 99.7%, CAS No. 67-64-1) and N,N-dimethylformamide (99.5%, CAS No. 68-12-2) were acquired from Samchun Chemicals. Disperse Yellow 54 (99%, CAS No. 12223-85-7) was supplied from Kyungin Corp. Disperse Blue 359 (>99%, CAS No. 62570-50-7) and Disperse Yellow 211 (>99%, CAS No. 86836-02-4) were supplied from Archroma Korea Corp. Disperse dyes from both suppliers were without any additives. Polyester double knit was provided from Shin Il Textile Co., Ltd. (150 D, 260 g/m²)

2.2 Apparatus for dissolution of dyes into scCO₂

The apparatus shown in Figure 5 was designed in order to measure the dissolution rate and solubility of each disperse dyes into scCO₂. From the CO₂ cylinder (1), vapor CO₂ was injected into the pre-cooler (3) where the temperature was controlled by the cooling bath (model: NCW-30M, Canatech Co., Ltd, South Korea) (2) to liquefy the CO₂ for easier pumping. Liquefied CO₂ then was pumped into the system using the CO₂ pump (model: HKS-12000, Hanyang Accuracy, South Korea) (4) to the reaction pressure of 250 bar. CO₂ that went through the CO₂ pump then entered the pre-heater (6) where the temperature was set by the heating bath (model: CW-05GL, Lab Companion, South Korea) (9) to the reaction temperature of 393 K. Then, scCO₂ was pumped into the dissolution cell (7) which was loaded with each dyes and the valve on top of the dissolution cell (7) was closed once the pressure inside the cell reached 250 bar. To maintain the temperature of the pre-heater (6) and dissolution cell (7) at a steady level, air bath (5) was used to keep the temperature inside the air bath to 373 K. On the both side of the dissolution cell (7), there were two optical sapphire windows for the light pathway from the

UV-Vis spectrophotometer (8) which is shown in yellow dotted lines in Figure 5. In order to measure the solubility and the dissolution rate of the dyes, in-situ UV-Vis spectrophotometer (model: AvaSpec-ULS2048L-EVO-RS, Avantes, Netherland) (8) was used to observe the absorbance. The measured absorbance from the UV-Vis spectrophotometer was then used to obtain the dissolution rate using AvaSoft 8 from Avantes.



1. CO₂ cylinder; 2. Cooling bath; 3. Pre-cooler; 4. CO₂ pump;
 5. Air bath; 6. Pre-heater; 7. Dissolution cell;
 8. UV-Vis spectrophotometer; 9. Heating bath;

Figure 5. In-situ UV-Vis apparatus for measurement of dissolution rate and solubility of dyes into scCO₂.

2.3 Apparatus for supercritical dyeing

The apparatus for the SCD process is very similar to the one used for the measurement of the dissolution rate except the dissolution cell (7) is replaced with a dyeing bath which does not contain two optical sapphires for UV-Vis spectrophotometer. Following the same method presented in Section 2.2, from the CO₂ cylinder (1), vapor CO₂ was transformed into scCO₂ through pre-cooler, pre heater, and pump following the same procedure as described in Section 2.2. For the SCD process, however, the scCO₂ was pumped into the dyeing bath of 44 mL. The dyeing bath was pre-loaded with each dyes and PET and was stirred using magnetic stirrer (model: Standard Telemodul, Thermo Fisher Scientific, U.S.A.). After the process was completed, the purge valve was used to depressurize the system.

2.4 Apparatus for extraction of impregnated dye

The impregnated dyes are not chemically bonded to the fabric but rather physically trapped. To measure the amount of the impregnated dyes inside the PET, therefore, PET must be swelled prior to extraction. Swelling and extraction of the dye was done using the apparatus shown in Figure 6 using N,N-Dimethylformamide as the solvent.



Figure 6. Soxhlet extractor used to extract the impregnated dye inside the PET at various time. [19]

2.5 Analytical methods

2.5.1 Measurement of the dissolution rate and solubility

Dissolution rate of each disperse dye was measured from the absorbance curve at the wavelengths corresponding to each color which were 440~450, 425~435, and 650~660 nm for DY54, DY211, and DB359 respectively. From the curves, scCO₂ was assumed to be saturated with dyes after the absorbance reached a steady value and the concentration of the dye at this value was defined as the solubility of the dye. Absorbance at a specific time, A_t , can be converted to concentration and thus, to amount of dissolved dye using the Beer-Lambert equation shown below.

$$A_t = \varepsilon * l * C \quad (1)$$

From the absorbance curve and the solubility of each dye which correspond to the equilibrium dye concentration, A_∞ , degree of saturation which is in Eqs. 2 was plotted against time in order to obtain the dissolution rate for each dye.

$$\text{Degree of saturation} = \frac{A_t}{A_\infty} \quad (2)$$

2.5.2 Measurement of the dye uptake

To measure the amount of impregnated dye inside the PET, SCD processed PETs were subjected to soxhlet extraction using N,N-dimethylformamide (DMF) as the solvent. After all the dyes were extracted from the PET, graduated cylinder was used to measure the volume of each DMF solution. Then, UV-Vis Spectrophotometer (Model: Evolution 201, Thermo Fisher Scientific, U.S.A.) was used to obtain the absorbance peak for each of the DMF solution. Using the Beer-Lambert equation, absorbance at any given time can be converted into concentration of the dye per volume of solution which combined with volume of the solution can give the mass of impregnated dyes at a specific time. Dye uptake was defined as Eqs. 3 and after three hours of dyeing, the dye uptake was assumed to reach a steady value and the value at this point was defined as the equilibrium dye uptake.

$$\text{Dye uptake (wt\%)} = \frac{\text{Mass of dye}}{\text{Mass of PET}} \quad (3)$$

$$\text{Equilibrium Dye uptake (wt\%)} = \frac{\text{Mass of dye at 3 h}}{\text{Mass of PET}} \quad (4)$$

Chapter 3. Results and discussion

3.1 Dye uptake

Prior to determining the rate of overall dyeing process, dye uptake of PET for the three disperse dyes were experimentally measured by first dyeing the fabric for specific time span followed by extracting the impregnated dye by soxhlet extractor. The equilibrium dye uptake for each disperse dyes were measured following the same procedure but dyeing was carried out until the dye uptake reached a plateau. As shown in Figure 7, the dye concentration inside PET reached the maximum after one hour for DB359 but kept on increasing for both DY54 and DY211 even after three hours. PETs treated at the reaction conditions for over three hours, however, seemed to went through deformation(ref) which was apparent during the soxhlet extraction where solvent was unsuccessful at extracting all the dyes inside the fabric. Due to the previous reasons, all dyeing experiments were conducted until three hours and the dye uptake at this point was assumed to be the equilibrium dye uptake.

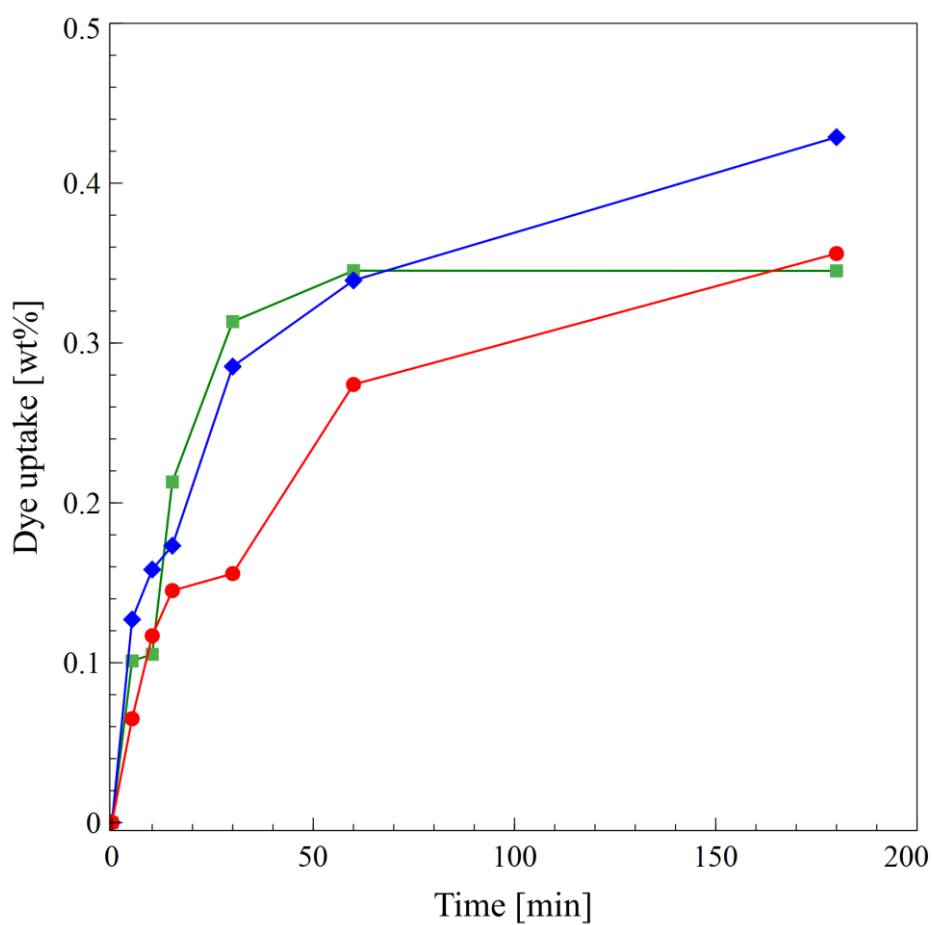


Figure 7. Dyeing rate for various dyes at 393 K & 250 bar from 0 to 180 min. DY54 (♦), DY211 (●), and DB359 (■) were assumed to be fully saturate the fabric at 180 min and the concentration at this time was defined as equilibrium dye uptake.

3.1.1 Solvent selection for soxhlet extraction

To measure the dye uptake at various time, dyed fabric was subjected to soxhlet extraction (Figure 6) followed by analysis using UV-Vis spectrophotometer respectively DMF was chosen as the solvent for soxhlet extraction for few reasons. The impregnated dyes were not chemically bonded to the fabric but rather physically trapped inside the polymer matrix. To extract the dyes inside the polymer matrix, thus, extraction must be carried out at the temperature higher than the glass transition temperature of the PET (~343 K) [20]. By using DMF, not only swelling can be easily achieved due to DMF's boiling point of 423 K but also the experimental temperature can be controlled below 473 K where degradation of the PET or disperse dyes can also take place [21]. UV-Vis spectrophotometer was used to obtain the absorbance spectrum of each DMF solution containing disperse dyes which in turn can be converted into amount of impregnated dye.

3.2 Calculation of the solubility parameter, δ

Prior to comparing the equilibrium dye uptake to other experimental results, solubility parameter, δ , of the PET, scCO₂, and disperse dyes of interest were obtained through previous studies.[22,23] Karst et al. reported solubility parameter data of various disperse dyes calculated from the Hildebrand method. For DB359 where the value was not obtained by Karst, the solubility parameter was calculated from the same method that was used for others which are shown in Table 2. The method used to calculate δ is known as the group contribution method where contribution of each functional group and fragment of the parent structure to the molar volume and the cohesive energy of the species is taken into consideration.[22] Eqs. 5 along with the estimated values of molar volume and cohesive energy for each fragment were used to calculate δ for the PET, scCO₂, and three disperse dyes. [22,24]

$$\delta = \left(\frac{\sum E_{cohesive_i}}{\sum V_{m_i}} \right)^{1/2} \quad (5)$$

Table 2.

Solubility of parameter, δ , of scCO₂, PET, DY54, DY211, and DB359. [22, 25, 27]

	δ [(J/cm ³) ^{0.5}]
scCO ₂ (393 K, 250 bar)	7.55
PET	30.9
DY54	30.8
DY211	27.6
DB359	29.2

3.2.1 Dissolution of dyes into CO₂

To determine the rate determining step of the overall dyeing process, the first step of dyeing which is the dissolution of dyes into scCO₂ has been studied. Key factors during dissolution is the rate of dissolution and the solubility of dyes to scCO₂. Both the solubility and dissolution rate was measured using in-situ UV-Vis spectrophotometer in the experimental conditions identical to the dyeing process (Figure 8). Measurements were taken as soon as CO₂ was introduced to the cell and stopped after absorbance spectrum reached a steady value. As shown in Figure 9, CO₂ was fully saturated with all the dyes of interest before 30 minutes, whereas equilibrium dye uptake was not reached at the same time span, implying dissolution may not be the limiting factor in the overall dyeing process.

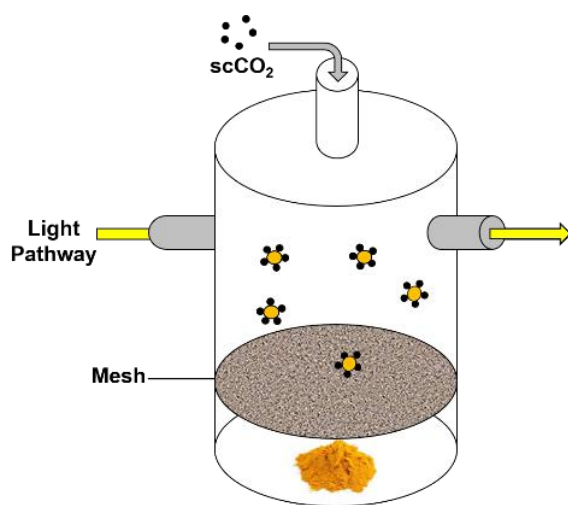


Figure 8. In-situ UV-Vis Spectrophotometer for the measurement of solubility and dissolution rate at 393 K, 250 bar.

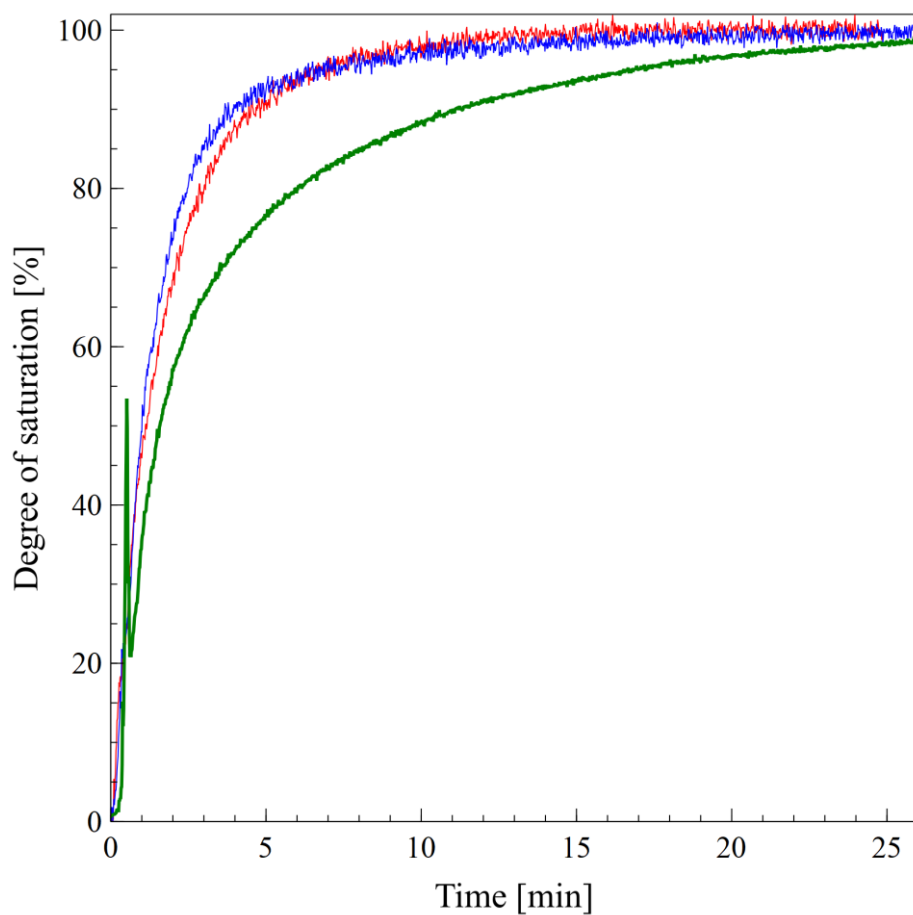


Figure 9. Dissolution rate of disperse dyes in scCO_2 measured from in-situ UV-Vis Spectrophotometer at 393 K, 250 bar. scCO_2 was assumed to be fully saturated with DY54 (—), DY211 (—), and DB359 (—) prior to 25 min.

3.2.2 Mass transfer to polymer surface

The next major step after dissolution of dye in scCO₂ is the mass transport of the dye-scCO₂ mixture from the bulk to the surface of PET. During the dyeing process, identical set of magnetic stirrer and stirring plate was used at the fixed rpm. Also, since the solubility of dyes of interest is very small with the order of magnitude of 10^{-4} ~ 10^{-2} , dye-scCO₂ mixture will have the physical properties very similar to the scCO₂. Following the logic, mass transfer to the polymer surface was assumed to be constant for all dyes throughout the experiment and the effect of mass transfer on the overall dyeing rate should be negligible.

Table 3.

Solubility of disperse dyes in scCO₂ at 393 K, 250 bar. [25]

Dye	Solubility [10^{-4} g dye/g CO ₂]
DY54	9.20
DY211	254
DB359	6.66

3.3 Diffusion of dyes inside the polymer matrix

While keeping the mass transfer of dye-scCO₂ mixture to the polymer surface constant and from the results shown in Section 3.2.1, it was reasonable to suspect that the diffusion of dyes inside the PET was the rate determining step of the overall dyeing process. To examine the hypothesis, dye uptake for each dyes was plotted in Figure 10 against $\sqrt{D_{AB}t}$ where D_{AB} is the diffusion coefficient of dye inside PET and t is the reaction time. For diffusion in a semi-infinite medium in cylinder, the total number of moles of solute, N_A , can be obtained starting from Fick's second law for one-dimensional diffusion and appropriate boundary conditions. C_A is the concentration of A inside the medium. [26]

$$\frac{\partial C_A}{\partial t} = \frac{D_{AB}}{r} \frac{\partial}{\partial r} \left(r \frac{\partial C_A}{\partial r} \right) \quad (6)$$

$$t \leq 0, \quad C_A = C_{A_0} \text{ for } r \geq 0, \quad (\text{BC } 1)$$

$$t > 0, \quad C_{A_{surface}} > C_{A_0} \text{ for } r = 0, \quad (\text{BC } 2)$$

$$r \rightarrow \infty, \quad C_A = C_{A_0} \text{ for } t \geq 0 \quad (\text{IC } 1)$$

Using Eqs.6 and Laplace transform, fractional concentration change, θ , can be shown as Eqs.7.

$$\theta = \frac{C_A - C_{A_0}}{C_{A_{surface}} - C_{A_0}} = \operatorname{erfc}\left(\frac{r}{2\sqrt{D_{AB}t}}\right) \quad (7)$$

Instantaneous rate of mass transfer across the surface of the medium can be expressed as below by taking the derivative of Eqs. 7 and combining with Fick's first law. Then, using the Leibnitz rule, n_A can be shown as Eqs.9.

$$n_A = -D_{AB}A\left(\frac{\partial C_A}{\partial r}\right)_{z=0} \quad (8)$$

$$n_{AZ=0} = \sqrt{\frac{D_{AB}}{\pi t}}A(C_{A_{surface}} - C_{A_0}) \quad (9)$$

From above, it can be shown that the total number of moles of solute, N_A , is proportional to $\sqrt{D_{AB}t}$ by integrating Eqs. 9 with respect to time which can be seen from the experimental data in Figure 10.

$$N_A \propto \sqrt{D_{AB}t}$$

From the SEM image of the fabric that was used throughout the experiment and the proportional relationship between N_A and D_{AB} , it was possible to assume the dyeing of the PET was done in the similar fashion to the unsteady state diffusion in semi-infinite medium for cylindrical system.

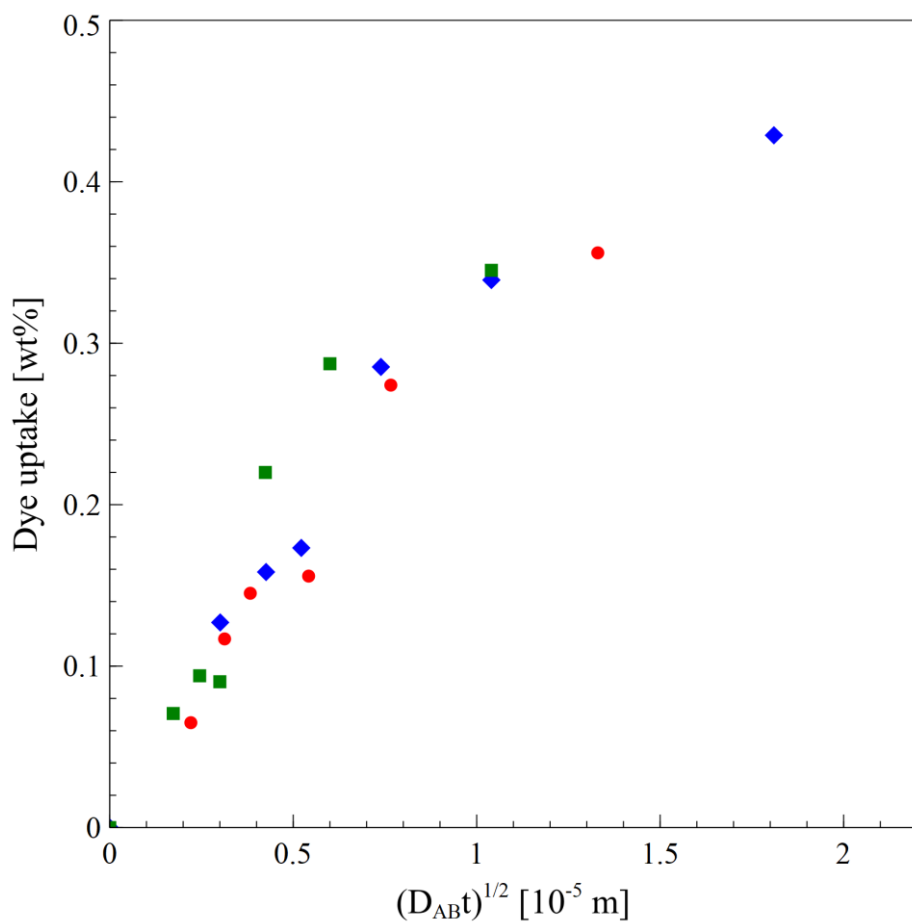


Figure 10. Correlation between the dye uptake and $(D_{AB}t)^{1/2}$ for DY54 (◆), DY211 (●), and DB359 (■) at 393 K, 250 bar from 0 to 180 min.

To find the governing equation to predict the rate of supercritical dyeing, Fick's second law for one-dimensional diffusion can be used again for cylinder of $r = a$ along with the following boundary and initial conditions.

$$r = a, \quad C_A = C_0 \text{ for } t \geq 0 \quad (\text{BC } 4)$$

$$0 < r < a, \quad C_A = f(r) \text{ for } t = 0 \quad (\text{BC } 5)$$

If initially the cylinder had a uniform concentration of $f(r) = C_1$ which is zero for this study, the analytical solution to the Eqs. 6 can be obtained which when integrated in terms of the concentration from $r = 0$ to $r = a$, gives the equation to predict the dye concentration at any given time.

$$\frac{C - C_1}{C_0 - C_1} = \frac{C}{C_0} = 1 - \frac{2}{a} \sum_{n=1}^{\infty} \frac{\exp(-D_{AB}\alpha_n^2 t) J_0(r\alpha_n)}{\alpha_n J_1(a\alpha_n)} \quad (10)$$

$$\frac{M_t}{M_{\infty}} = 1 - \sum_{n=1}^{\infty} \frac{4}{a^2 \alpha_n^2} \exp(-D_{AB}\alpha_n^2 t) \quad (11)$$

where M_t is the mass of impregnated dye inside the polymer at time t and M_{∞} is the equilibrium dye uptake. For this experiment, Eqs. 11 was chosen as the governing equation and by using it, dyeing rate predicted by the equation and the experimental results were compared as shown in Figure 12 through 14. From the figures, it can be observed that the governing equation apparently overestimated the dying rate for all the dyes of interest and the deviation of the experimental data from the governing equation may be the result of few factors.

Derivation of the governing equation assumed the surface concentration at $t = 0$ to be C_0 . It can be observed, however, from Figure 9 that the scCO_2 is not fully saturated with any of the dye until 20 to 30 minutes of dissolution time. Until the equilibrium concentration is reached, concentration at the surface will always be less than C_0 which will in turn result in less dyeing at a given time. It can be seen from Figure 12 to 14 where the expected curve for C_0 , $0.75C_0$ and $0.5C_0$ were plotted, that lower value of C_0 will in fact shift the expected curves and thus, lower the mass of impregnated dyes inside the PET. In a similar logic, C_0 was not achieved at $t = 0$ but rather some time after the dyeing. If by letting $t = 0$ the time where $C = C_0$, the experiment could be considered as having certain time lag. Both lower C_0 and time lag will result in curve shift which aligned with the experimental results and thus, it is possible to propose that if the dissolution of the dyes was completed in much shorter span of time, the experimental results would have less deviation from the expected curve obtain from the governing equation.

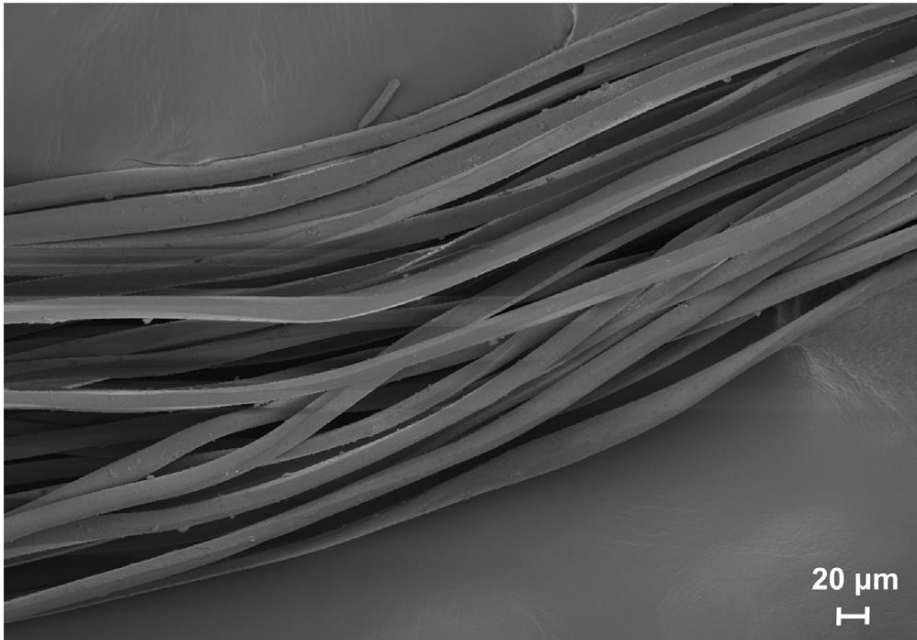


Figure 11. SEM image of the PET used throughout the experiments. [28]

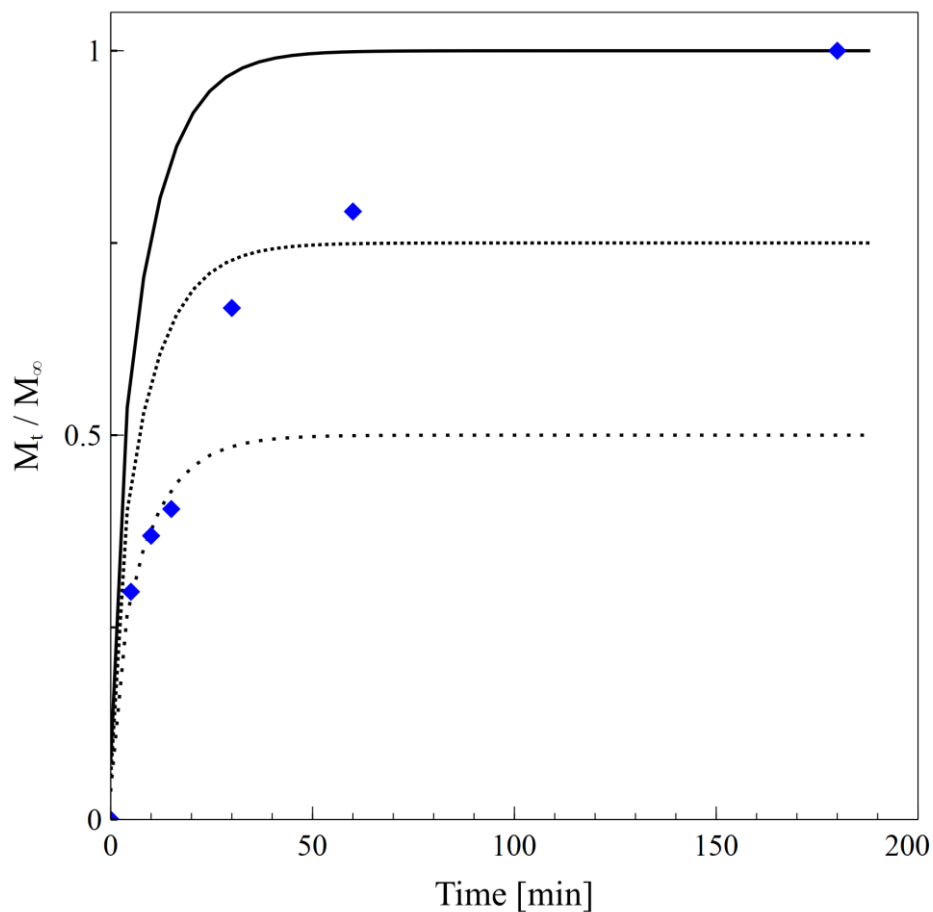


Figure 12. Rate of dyeing for DY54. Expected values from the governing equation and experimental values of DY54 (♦) are plotted. The solid line represents the expected results for C_0 and the other two dashed lines for $0.75C_0$ and $0.5C_0$ respectively.

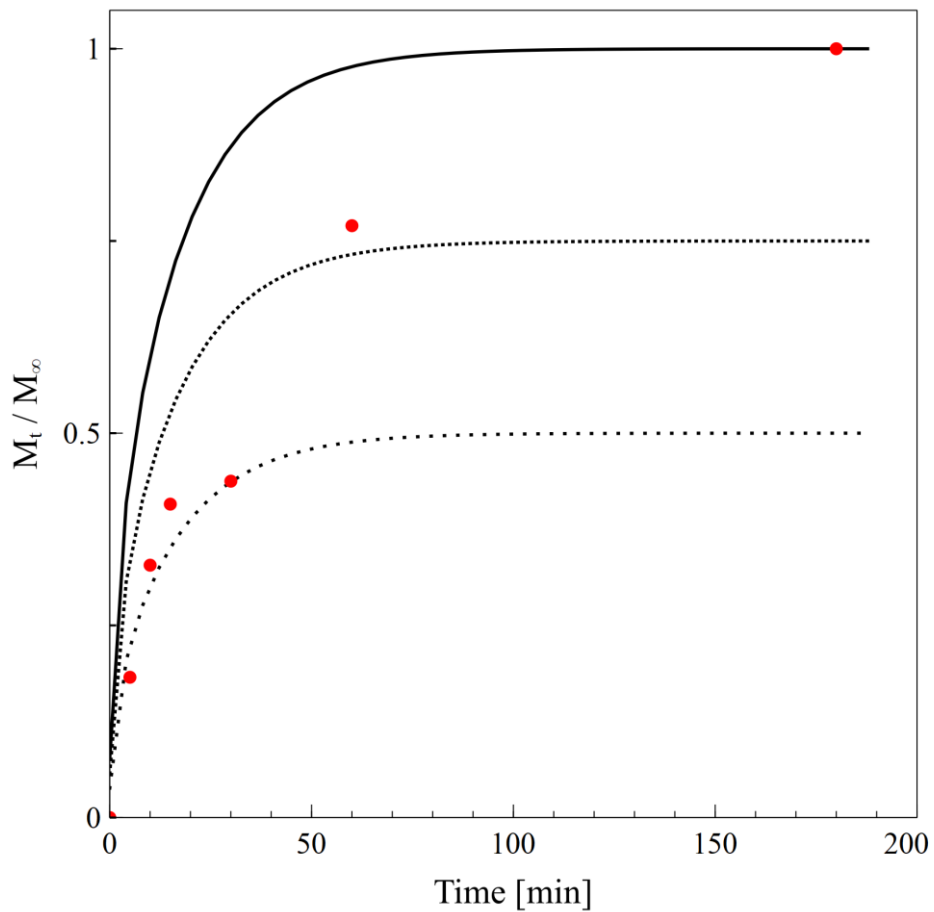


Figure 13. Rate of dyeing for DY211. Expected values from the governing equation and experimental values of DY211 (●) are plotted. The solid line represents the expected results for C_0 and the other two dashed lines for $0.75C_0$ and $0.5C_0$ respectively.

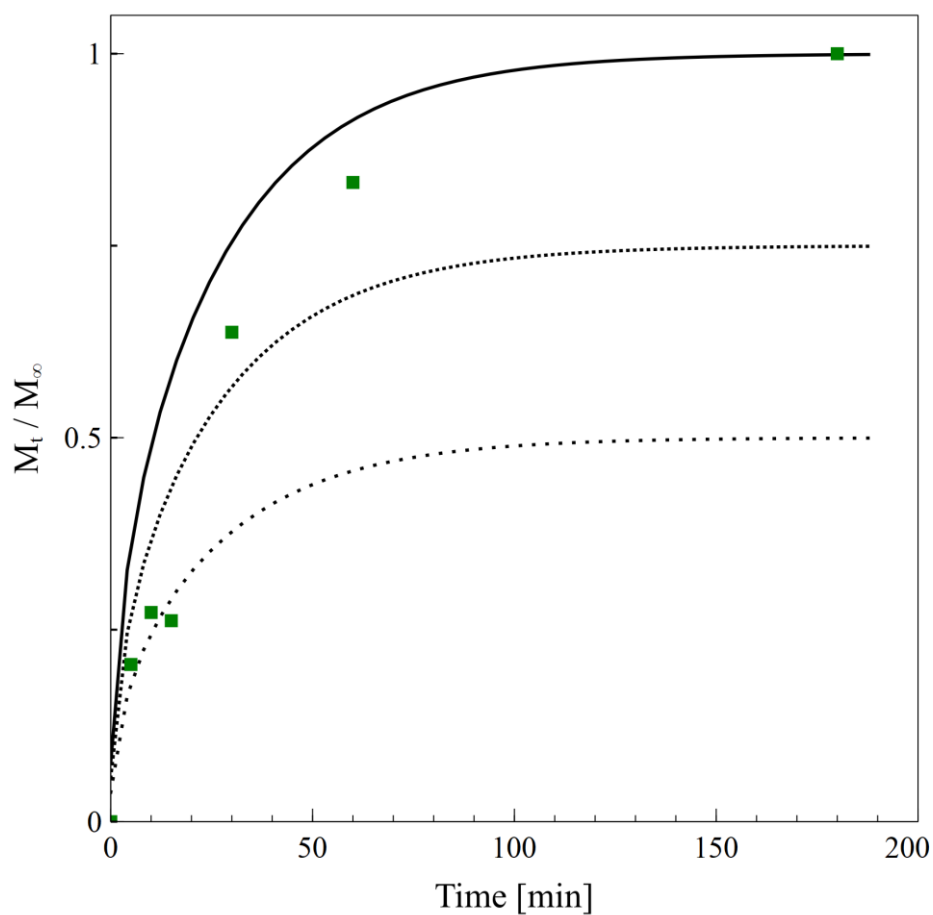


Figure 14. Rate of dyeing for DB359. Expected values from the governing equation and experimental values of DB359 (■) are plotted. The solid line represents the expected results for C_0 and the other two dashed lines for $0.75C_0$ and $0.5C_0$ respectively

Chapter 4. Conclusion

In this work, the kinetics of the overall supercritical dyeing process using scCO_2 , PET, and three different disperse dyes was studied in order to find the governing parameter for the entire process. To investigate the effect of each parameter on the dyeing kinetics, overall SCD process was divided into three major steps: dissolution of the dye into the scCO_2 , mass transport of the dye- scCO_2 solution to the fabric, and diffusion of the dye inside the polymer matrix. Throughout the experiment, the mass transport of dye- scCO_2 was assumed to be constant for the three dyes and thus the effect of it was negligible. After 20 minutes, scCO_2 was saturated with all the dyes whereas the equilibrium dye uptake kept on increasing until three hours. It was assumed, therefore, that the diffusion inside the polymer matrix is the rate determining step for the overall SCD. The hypothesis was tested and proved to be valid from the plot of overall dye uptake vs. $\sqrt{D_{AB}t}$ where the dye uptake was proportional to $\sqrt{D_{AB}t}$. The proportional behavior of the dye uptake with respect to $\sqrt{D_{AB}t}$ implied the overall SCD occurs in the similar fashion to the unsteady-state mass transfer in

semi-infinite medium for cylinder. From the assumption that the overall SCD is in fact similar to the one mentioned above, the governing equation was obtained from the Fick's second law for one-dimensional diffusion for cylinder with appropriate initial and boundary conditions. Experimental results showed deviation from the governing equation which could have caused by the time delay it took for the scCO₂ to be fully saturated with the dyes. The governing equation assumed that the dye dissolved in scCO₂ was at its maximum whereas it took 20 to 30 minutes to reach saturation. As a result of lower concentration of dye inside the scCO₂, the dye uptake at certain point may have been lowered which explains the deviation of the experimental values from the expected ones. Apart from the deviation, the assumption that the diffusion of the dyes inside the fabric is the rate determining step seemed logical. Thus, rough estimates of the dyeing kinetics of untested dyes with known diffusion coefficient can be obtained through one or two experiments followed by comparison of the dye uptake to $\sqrt{D_{AB}t}$. A possible way to decrease the deviation shown in the result is to lower the dissolution time. Micronization of the dyes have been carried out by others using Supercritical Anti-Solvent (SAS) process or Rapid Expansion of Supercritical Solution (RESS) to enhance the stability and

increase the surface area. [29-32] Also, to further validate the hypothesis that were established throughout this study, experiments on other disperse dyes can be done under the same experimental conditions.

Bibliography

1. Kant, R., Textile dyeing industry an environmental hazard. *Natural Science* **2012**, 4 (1), 5.
2. Banchero, M., Supercritical fluid dyeing of synthetic and natural textiles - a review. *Color Technol* **2013**, 129 (1), 2-17.
3. Yasuji, T.; Takeuchi, H.; Kawashima, Y., Particle design of poorly water-soluble drug substances using supercritical fluid technologies. *Adv Drug Deliver Rev* **2008**, 60 (3), 388-398.
4. Palmer, M. V.; Ting, S. S. T., Applications for Supercritical-Fluid Technology in Food-Processing. *Food Chem* **1995**, 52 (4), 345-352.
5. Kankala, R. K.; Zhang, Y. S.; Wang, S. B.; Lee, C. H.; Chen, A. Z., Supercritical Fluid Technology: An Emphasis on Drug Delivery and Related Biomedical Applications. *Adv Healthc Mater* **2017**, 6 (16).
6. Sahena, F.; Zaidul, I. S. M.; Jinap, S.; Karim, A. A.; Abbas, K. A.; Norulaini, N. A. N.; Omar, A. K. M., Application of supercritical CO₂ in lipid extraction - A review. *J Food Eng* **2009**, 95 (2), 240-253.
7. Ahn, Y.; Bae, S. J.; Kim, M.; Cho, S. K.; Baik, S.; Lee, J. I.; Cha, J. E., Review of Supercritical CO₂ Power Cycle Technology and Current Status of Research and Development. *Nucl Eng Technol* **2015**, 47 (6), 647-661.
8. Park, S. C.; Tuma, D.; Kim, S.; Lee, Y. R.; Shim, J. J., Sorption of C. I. Disperse Red 60 in polystyrene and PMMA films and polyester and Nylon 6 textiles in the presence of supercritical carbon dioxide. *Korean J Chem Eng* **2010**, 27 (1), 299-309.
9. Ngo, T. T.; Liotta, C. L.; Eckert, C. A.; Kazarian, S. G., Supercritical fluid impregnation of different azo-dyes into polymer: in situ UV/Vis spectroscopic study. *J Supercrit Fluid* **2003**, 27 (2), 215-221.
10. Miyazaki, K.; Tabata, I.; Hori, T., Relationship between colour fastness and colour strength of polypropylene fabrics dyed in supercritical carbon dioxide: effect of chemical structure in 1,4-

bis(alkylamino)anthraquinone dyestuffs on dyeing performance. *Color Technol* **2012**, *128* (1), 60-67.

11. Long, J. J.; Xiao, G. D.; Xu, H. M.; Wang, L.; Cui, C. L.; Liu, J.; Yang, M. Y.; Wang, K.; Chen, C.; Ren, Y. M.; Luan, T.; Ding, Z. F., Dyeing of cotton fabric with a reactive disperse dye in supercritical carbon dioxide. *J Supercrit Fluid* **2012**, *69*, 13-20.

12. Guzel, B.; Akgerman, A., Mordant dyeing of wool by supercritical processing. *J Supercrit Fluid* **2000**, *18* (3), 247-252.

13. Abou Elmaaty, T.; Abd El-Aziz, E., Supercritical carbon dioxide as a green media in textile dyeing: A review. *Text Res J* **2018**, *88* (10), 1184-1212.

14. Zhang, R. R.; Ma, X. T.; Shen, X. X.; Zhai, Y. J.; Zhang, T. Z.; Ji, C. X.; Hong, J. L., PET bottles recycling in China: An LCA coupled with LCC case study of blanket production made of waste PET bottles. *J Environ Manage* **2020**, 260.

15. Zander, N. E.; Gillan, M.; Lambeth, R. H., Recycled polyethylene terephthalate as a new FFF feedstock material. *Addit Manuf* **2018**, *21*, 174-182.

16. Taniguchi, I.; Yoshida, S.; Hiraga, K.; Miyamoto, K.; Kimura, Y.; Oda, K., Biodegradation of PET: Current Status and Application Aspects. *Acs Catal* **2019**, *9* (5), 4089-4105.

17. von Schnitzler, J.; Eggers, R., Mass transfer in polymers in a supercritical CO₂-atmosphere. *J Supercrit Fluid* **1999**, *16* (1), 81-92.

18. Gupta, R. B. S., J. J., *Solubility in Supercritical Carbon Dioxide*. CRC Press: 2007.

19. Kasiri, M. B. S., S., Exploring and exploiting plants extracts as the natural dyes/antimicrobials in textiles processing. *Progress in color, colorants and coatings* **2015**, *8*, 28.

20. Jog, J. P., Crystallization of Polyethyleneterephthalate. *J Macromol Sci R M C* **1995**, *C35* (3), 531-553.

21. Kim, T. 초임계 염색 공정에서 폴리에스터 섬유 내 분산 염료 확산 거동 예측에 관한 연구. Seoul National University, 2020.

22. Karst, D.; Yang, Y. Q., Using the solubility parameter to explain disperse dye sorption on polylactide. *J Appl Polym Sci* **2005**, 96 (2), 416-422.
23. Martin, A.; Newburger, J.; Adjei, A., Extended Hildebrand Solubility Approach - Solubility of Theophylline in Polar Binary Solvents. *J Pharm Sci* **1980**, 69 (5), 487-491.
24. Fedors, R. F., Method for Estimating Both Solubility Parameters and Molar Volumes of Liquids. *Polym Eng Sci* **1974**, 14 (2), 147-154.
25. 산업통상자원부 200kg 급 초임계유체염색설비 및 염색공정기술 개발_2차년도 기술개발 내용; DYETEC연구원, Seoul National University, Yeungnam University: 2018.
26. Crank, J., *The Mathematics of Diffusion*. 2 ed.; Oxford University Press: 1975.
27. NIST, NIST Chemistry WebBook.
28. Kim, T.; Seo, B.; Park, G.; Lee, Y. W., Predicting diffusion behavior of disperse dyes in polyester fibers by a method based on extraction. *J Supercrit Fluid* **2020**, 157.
29. Kim, T.; Seo, B.; Park, G.; Lee, Y. W., Effects of dye particle size and dissolution rate on the overall dye uptake in supercritical dyeing process. *J Supercrit Fluid* **2019**, 151, 1-7.
30. Reverchon, E.; Adami, R.; De Marco, I.; Laudani, C. G.; Spada, A., Pigment Red 60 micronization using supercritical fluids based techniques. *J Supercrit Fluid* **2005**, 35 (1), 76-82.
31. Wu, H. T.; Lee, M. J.; Lin, H. M., Precipitation kinetics of pigment blue 15 : 6 sub-micro particles with a supercritical anti-solvent process. *J Supercrit Fluid* **2006**, 37 (2), 220-228.
32. Wu, H. T.; Lin, H. M.; Lee, M. J., Ultra-fine particles formation of C-1. Pigment Green 36 in different phase regions via a supercritical anti-solvent process. *Dyes Pigments* **2007**, 75 (2), 328-334.

국 문 초 록

서울대학교 대학원

공과대학 화학생물공학부

김 동 준

현대 사회에서 천의 사용은 섬유 산업뿐만 아니라 다양한 사업 부문에서 큰 비중을 차지하고 있다. 따라서 천에 대한 다양한 분야에서의 연구가 선행되었고 그중에서 PET의 염색은 PET의 많은 사용량 때문에 많은 관심이 집중되고 있다. PET의 염색은 기존의 수계 염색뿐만 아니라 초임계이산화탄소를 이용한 초임계 염색으로도 염색할 수 있다. 초임계염색은 크게 염료의 초임계이산화탄소로의 용해, 용해된 염료가 섬유의 표면으로 이동하는 물질전달 그리고 섬유 내에서 분산염료의 확산으로 나눌 수 있다. 본 연구는 온도와 압력에 따른 변화를 최소화하기 위해 기존 선행연구들에서 많이 쓰이는 393K, 250bar에서 진행되었고 총 3가지 분산염료를 (Disperse Yellow 54, Disperse Yellow 211,

Disperse Blue 359) 사용했습니다. 초임계염색공정을 총괄할 수 있는 변수를 찾기 위해 염료의 용해속도, 용해도, 용해도 계수, 염색량을 비교하였고 이를 통하여 염색량이 $\sqrt{D_{AB}t}$ 에 비례하는 결과를 얻을 수 있었다. 이를 통하여 전체 염색공정 중 섬유 내에서 염료의 확산이 속도 결정 단계라는 것을 확인할 수 있었고 이 가정을 통하여 속도식을 세울 수 있었다. 이후 세 가지 염료에 대한 염색량과 속도식을 비교를 통하여 속도식이 모든 염료에 대해서 염색량을 과대평가하는 것을 확인할 수 있었다. 반응을 시작할 때 이산화탄소는 염료에 포화된 상태라는 가정을 속도식을 구하기 위해 사용했지만 실제로는 이산화탄소가 포화농도에 도달하지 못한 것을 용해속도 실험을 통해서 알 수 있었다. 따라서 반응을 시작할 때 이산화탄소 내의 염료 농도가 속도식에 미치는 영향을 보기 위해 50%와 75%의 포화농도를 가정하여 속도식을 다시 구하였다. 염료의 농도가 50%와 75%이고 염색 시간이 짧을 때 실험값과 속도식이 작은 편차를 보였고 염색 시간이 길어질수록 실험값이 포화농도를 이용한 속도식과 비슷해지는 것을 확인할 수 있었다. 이를 통하여 용해속도를 증가시키면 실험값과 속도식으로 예측된 값이 작은 편차를 보일 것이라 예상할 수 있다. 따라서 위 방법으로

연계되는 속도식으로부터 새로운 염료에 대한 속도식을 예측할 수 있을 것이라 생각한다.